OCT Image Inspections of Indicator Plant Leaves Under Environmental Stresses

Hayate Goto[a] and Tatsuo Shiina[b]
Graduate School of Science and Engineering, Chiba University,
1-33 Yayoi-cho, Inage-ku, Chiba-shi, Chiba, 263-8522, Japan

Keywords: Optical Coherence Tomography, Indicator Plant, Environmental Assessment, Water Stress, Ozone Stress.

Abstract: In recent years, environmental pollution has intensified, raising concerns about the health impacts on humans and plants. In this study, we evaluate the indicator plants that can indicate environmental conditions by Optical Coherence Tomography (OCT) which can make tomographic images quantitatively and non-invasively observation. *Trifolium repens*, commonly known as white clover, which is prevalent in Japan, serves as an indicator plant for ozone, suggesting that OCT measurements of *Trifolium repens* enabled the estimation of ozone concentration. However, to evaluate whether the changes observed inside leaves are specific to ozone, it is necessary to also differentiate other environmental stresses. In this study, we compared the OCT measurement results of *Trifolium repens* grown under ozone stress and water stress. The analysis focused on variations in tissue thickness, interference light intensity, and texture of the OCT images, while also considering the stability of the analytical parameters. Differences were observed in the trends of changes in palisade tissue thickness and interference light intensity under ozone stress and water stress. Although variations under those stresses were observed in the results of texture analysis, these were not as significant as those in thickness and intensity. This result indicates that plants induce specific changes within their leaves due to different stresses, confirming the potential of OCT measurements for environmental assessments.

1 INTRODUCTION

In recent years, the progression of environmental pollution has become a problem in urban and industrial areas. In particular, ozone, produced when gases emitted from vehicles react with sunlight, can become concentrated enough high to harm plants and animals in the present automobile-advanced society. To estimate environmental conditions, there is a method that involves observing indicator plants that are sensitive to specific or multiple environmental stress factors(Kitao et al., 2009; Oishi, 2018). By measuring indicator plants, it is possible to infer the stress conditions to which the plants are exposed, enabling a comprehensive evaluation of the surrounding environment. This approach provides critical data that can be utilized for the effective control of both the quality and quantity of crop production. The observation of indicator plants typically relies on non-quantitative methods, such as visual inspections or microscopic examinations, which require pre-treatment that damages the plants. Although these methods provide insights into environmental conditions, the development of remote sensing techniques capable of quantitatively assessing plant responses without altering their internal states is essential. In this study, we used OCT (Optical Coherence Tomography), which can quantitatively measure and visualize the internal structure of a sample in a non-invasive, non-contact, and non-destructive manner(Fercher et al., 1996).

OCT has been studied and developed in the fields of ophthalmology (Tewarie et al., 2012), dentistry(Colston et al., 1998; Schneider et al., 2017), and dermatology (Liu et al., 2020). Research has been especially active in the field of ophthalmology, where the technology is useful for the diagnosis of glaucoma through visualization of the retina. It has also been studied in the field of agriculture and has been used to diagnose fruit diseases (M. Li et al., 2021; Sharifi et al., 2023), monitor seed germination (X. Li et al., 2022), and monitor crops during storage (Srivastava et al., 2018). In addition to measurements in the laboratory, research has also been done to carry the devices to plant growth sites to measure live plants without damaging them by cutting (Lee et al., 2019). We have developed TD-OCT(Time-Domain OCT) plant measurement system (Goto, Lagrosas, & Shiina, 2024; Goto, Lagrosas, Galvez, et al., 2024; Goto & Shiina, 2023).

[a] https://orcid.org/0000-0001-5387-9109
[b] https://orcid.org/0000-0001-9292-4523

The objective of this study is to evaluate the ozone status of the surrounding environment to which *Trifolium repens*, an ozone indicator plant, is exposed using feature extraction by OCT measurements. When plant leaves are exposed to ozone gas, ozone enters the leaf through the stomata, producing reactive oxygen species that destroy the palisade tissue (the regularly arranged tissue located inside the leaf close to the adaxial epidermis, which is the front side of the leaf)(Pell et al., 1997). In the case of water stress, stomatal occlusion occurs to inhibit transpiration from the stomata. As a result, the amount of CO_2 taken in through the stomata is reduced and photosynthesis is suppressed(Osakabe et al., 2014). Thus, when leaves are exposed to different stresses, different responses are triggered within the leaf. Therefore, in OCT measurements of stress-injured leaves, OCT images will reflect different characteristics for each stress. In this study, we analyse OCT images of leaves exposed to ozone stress and water stress, and discuss the feature extraction that appeared in those leaves. This study will verify that OCT measurements can provide a comprehensive observation of the surrounding environmental conditions to which leaves are exposed.

2 METHOD

2.1 Optical Coherence Tomography

The OCT (Optical Coherence Tomography) system developed in our laboratory for plant measurement is shown in Fig. 1. The system is based on TD-OCT with a Michelson interferometer configuration, and OCT measures the relative distance between interference points by identifying the backscattered position of light within the sample. The light from the SLD light source (central wavelength: 1310 nm, wavelength width: 53 nm) is split into two paths (reference path and sample path) by a fiber coupler. In the reference path, the optical path length changes at a constant speed due to a rotation mechanism and returns to the fiber coupler. In the sample path, the light backscattered at each layer of the sample returns to the fiber coupler with an optical path length corresponding to the backscattered position. The light returning from both paths interferes, and the intensity of the interference light is detected by an oscilloscope.

Since low-coherence light is used, the interference light intensity is obtained only when the optical path lengths of the two lights match within the coherence length. The reflecting position of the light within the sample is determined by the time difference between interference points, and the scanning speed of the optical path length of the reference arm(A-scan). Additionally, by moving the probe that irradiates the light parallel to the surface of the sample during measurement, two-dimensional information including internal information about the sample can be obtained (B-scan). A two-dimensional tomographic image can be created by mapping the intensity information with colors.
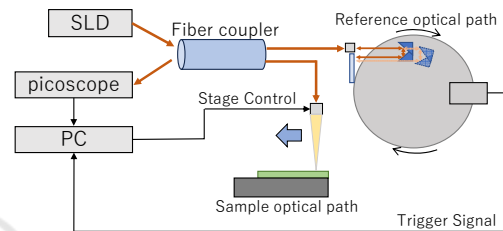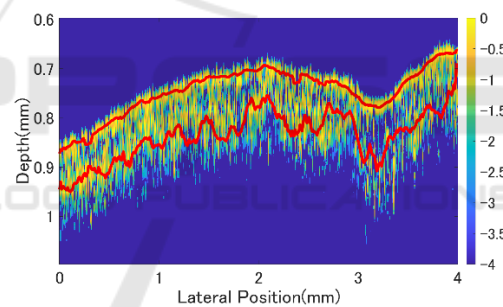

Figure 1: OCT configuration.

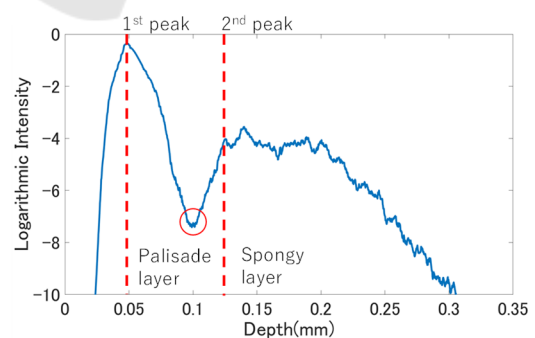Figure 2: Peak detection on OCT image.

Figure 3: Averaged A-line.

(a) Before exposure to water stress
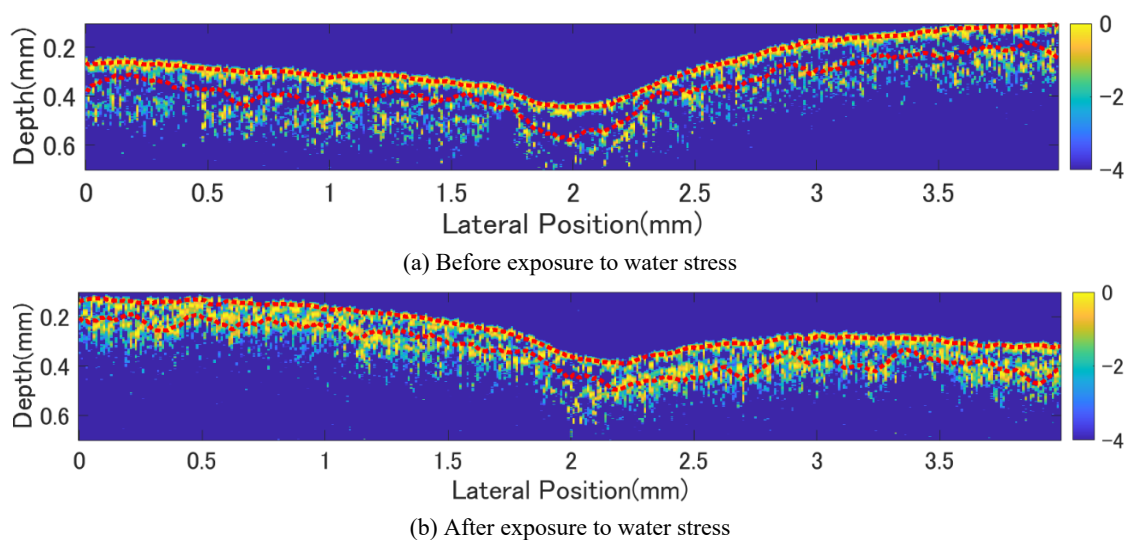

(b) After exposure to water stress

Figure 4: OCT images of leaves under water stress.

The axial resolution of the OCT is determined by the coherence length, which is determined by the central wavelength and wavelength width. Although the resolution increases as the central wavelength becomes shorter, the absorption of chlorophyll becomes stronger, resulting in a shallower depth. Therefore, a wavelength of 1310 nm was selected. The axial resolution calculated from the central wavelength and wavelength width is 14.2 μm. The output of the SLD is 15 μW, and the acquisition speed of the A-line is 25 Hz. During measurement, the OCT light is incident on the abaxial side of the leaf, and each A-line is averaged from 16 measurements to suppress noise. The B-scan image is created by acquiring 400 A-lines at intervals of 10 μm.

2.2 Signal Analysis

The acquired A-line signals were performed background light subtraction, intensity correction due to focal distance displacement, moving average, normalization, and logarithmic transformation. The intensity correction due to focal distance was performed to compensate for intensity attenuation caused by deviations from the focal distance. This correction applies the inverse of the focal intensity distribution that shows the interference light intensity changes due to the displacement from the focal position to the A-line.

Based on the analysis of the thickness, intensity, and texture of the palisade tissue from the B-scan image, comparisons of measurement results for each leaf were conducted. Initially, to obtain the location of the palisade tissue within the B-scan images, peak detection was performed for each A-line. The results of the peak detection are indicated by the red lines in Fig. 2. In the OCT image of leaves in Fig. 2, the vertical axis represents the depth direction of the leaf and the horizontal axis indicates the lateral position. The peak detection identified the first peak (the interface between the adaxial epidermis and the palisade tissue) and the second peak (the interface between the palisade tissue and the spongy tissue). The distance between the first and second peaks (representing the thickness of the palisade tissue) was calculated for each A-line, and the average thickness across the entire B-scan image was estimated. To acquire the intensity in the palisade tissue, all A-lines within the B-scan image were averaged to create a single A-line (Fig. 3). The minimum intensity obtained at the location of the palisade tissue from the peak detection was recorded as the intensity of the palisade tissue. Texture analysis was performed using the Gray Level Co-occurrence Matrix (GLCM). In GLCM, the number of pairs of intensity differences between adjacent pixels is counted to create a matrix, thereby extracting local variations within the image. From the constructed matrix, Contrast, Correlation, Energy, and Homogeneity were calculated. Contrast increases as the number of pixel pairs with large intensity differences in the image. Correlation becomes larger when pixel pairs have values closer to the matrix mean. Energy increases with a higher frequency of identical intensity pairs, while Homogeneity grows as the number of pixel pairs with similar intensities increases.
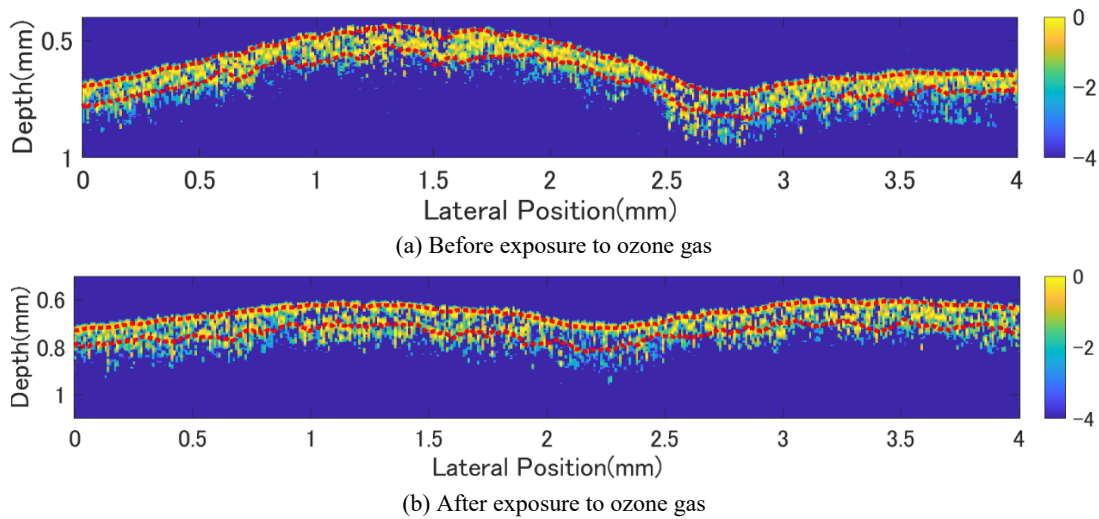
(a) Before exposure to ozone gas

(b) After exposure to ozone gas

Figure 5: OCT images of leaves under ozone stress.

2.3 Leaf Samples

The sample used in this study was the five leaves of *Trifolium repens* (White Clover), an indicator plant for ozone gas. The leaves were grown in an incubator maintained at a constant temperature of 25°C, with 12 hours of light exposure during the day.

In the water stress experiment, an automatic watering system was used. OCT measurements were taken for 11 days after stopping watering until the *Trifolium repens* wilted. Once the plants had wilted for 14 days, watering was resumed, and the leaf recovery process was observed by OCT.

For the ozone stress experiment, an ozone gas generator was placed in the incubator, and the plants were grown in an environment with an ozone concentration of approximately 0.2 ppm during the measurement period. This concentration can have significant influences on both humans and plants. Measurements were taken several times over 10 days after the ozone generator was introduced to monitor changes over time.

3 RESULT

3.1 Stress Influences on Leaves

The measurement results before and after applying water stress to the *Trifolium repens* leaves are shown in Fig. 4. In contrast, the results before and after ozone stress are shown in Fig. 5. In these images, the horizontal axis represents the lateral position of the OCT probe, and the vertical axis shows the depth of

the sample. The measurements were taken from the adaxial side of the leaves, representing the results when light was illuminated from the top of the images.

In Fig. 4(a), from top to bottom, the adaxial epidermis, palisade layer, and spongy layer are visible. The adaxial epidermis appears as a region of stronger signal intensity around a depth of 0.2 mm in Fig. 4(a). Below the epidermis, there is a region where the signal disappears and then reappears, indicating the presence of the palisade tissue, which is situated above the spongy layer.

After applying water stress, an increase in signal density is observed in the spongy layer. In Fig. 4(b), on the left side, the originally visible palisade tissue layer appears to have thinned, causing the signals from the adaxial epidermis and the spongy layer to merge. It seems to be little change in the main vein.

In contrast, after applying ozone stress, the signal density decreases in Fig.5(b), and the palisade layer becomes more distinct, showing changes opposite to those caused by water stress. Additionally, the main vein becomes less defined. Since OCT images make it difficult to perform quantitative assessments or objectively evaluate small changes, the variations in the images were quantified by analyzing the intensity, and thickness of the palisade tissue, and texture using GLCM (Gray Level Co-occurrence Matrix).

3.2 Intensity Change in Palisade Tissue

Figure 6 illustrates the changes in the intensity of the palisade tissue (red circles in Fig. 3) under the stresses. The horizontal axis of Fig. 6 represents the number of days since each type of stress was applied. The vertical axis represents the absolute intensity

value in the palisade tissue, where a higher value indicates less reflection from the palisade tissue. The blue dots represent the results of the water stress experiment, where the leaves wilted from day 11, and watering was resumed on day 14. The orange dots show the results of the ozone stress experiment(up to 10 days).

In the case of water stress, the values decreased during the period from when watering was stopped until the leaves wilted. Even after watering was resumed and the leaves recovered, the intensity of the palisade tissue remained unchanged, maintaining a nearly constant value. In contrast, the ozone stress experiment showed a gradual increase, although the change was not as significant as in the water stress experiment.

Under water stress, the cell walls likely hardened as a response to minimize the effects of the stress, which resulted in stronger reflections within the cells. Even after watering resumed, it is possible that the hardened cell walls did not fully recover during the measurement period. On the other hand, under ozone stress, ozone penetrated and damaged the cell walls, disrupting the organized structure of the palisade tissue, which likely reduced the amount of light reflected in the probe. The two types of stress caused different changes within the leaves, allowing us to evaluate these differences using OCT.

3.3 Thickness Change in Palisade Tissue

Figure 7 illustrates the changes in the thickness of the palisade tissue (between the two red lines in Fig. 2) under the stresses. The vertical axis of Fig. 7 represents the average thickness of the palisade tissue.

During the water stress period, a decrease in thickness was observed until wilting(day 11). This reduction is due to a decrease in internal water content, reducing cell volume. After watering was resumed, the thickness approached its original value, but there were few changes after that. These few changes, similar to the intensity measurements in the palisade tissue, indicate that the cell condition did not fully recover during the measurement period.

In contrast to water stress, the ozone stress experiment showed a gradual increase in thickness. This increase will be attributed to water filling the intercellular spaces by the disruption of the palisade tissue, resulting in swelling through osmotic pressure. As with the intensity measurements, the two types of stress resulted in distinct changes in the palisade tissue.
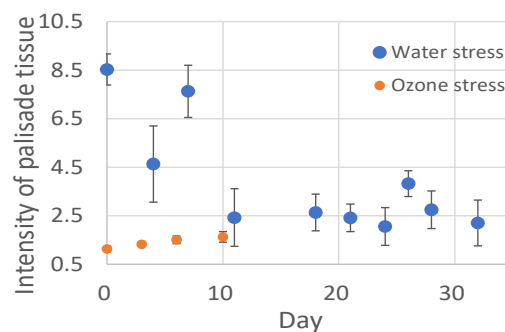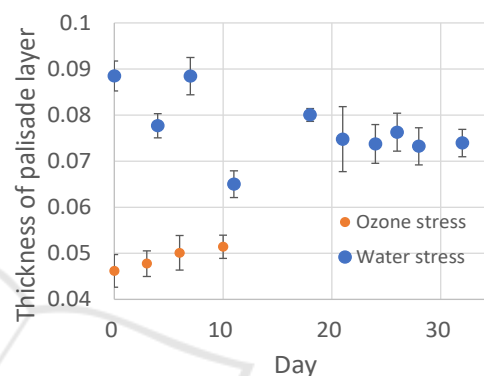

Figure 6: Intensity of palisade tissue.

Figure 7: Thickness of palisade layer.

3.4 Texture Change in Palisade Tissue

Figure 8 shows the GLCM measurement results before and after water stress and ozone stress. The horizontal axis indicates the number of days, while the vertical axis shows (a) Contrast, (b) Correlation, and (c) Homogeneity values, respectively.

During water stress, the Contrast decreased until wilting(Fig.8(a)). After watering was resumed, the Contrast temporarily returned to a value close to its original level but then decreased again, stabilizing at a certain value. The Contrast value is higher when there is a greater difference in intensity between adjacent pixels. In the case of water stress, the reduction in thickness of the palisade tissue in Fig.7 led to fewer regions with low signal intensity within the palisade tissue, resulting in a smaller intensity difference in Fig.4. The temporary increase in thickness after resuming watering will have contributed to the similar trend observed in the Contrast. In contrast, under ozone stress, the Contrast initially decreased but returned to its original value after 10 days. Ozone stress destroys the palisade tissue, causing light scattering within it to become random. This randomness contributed to the decrease in the signal from the palisade tissue. Additionally, when the leaf is damaged partially by ozone, it will be

increased the intensity differences, which causes the rise in Contrast observed after 10 days.

The Correlation values showed little change for both water stress and ozone stress(Fig.8(b)). After resuming watering, there was a temporary significant decrease in the value compared to other periods, but it returned to a level similar to the original within a few days. The Correlation value increases when there are similar structures in the image. Within the leaf, similar structures are repeated in the horizontal direction, causing this value to approach nearly equal to 1. Immediately after resuming watering, the partial recovery of only certain areas of the leaf can introduce some heterogeneity, resulting in a temporary decrease in the Correlation value.
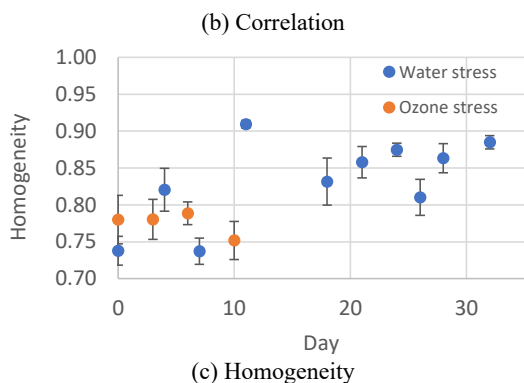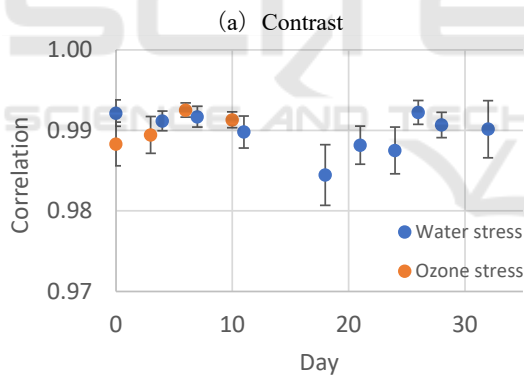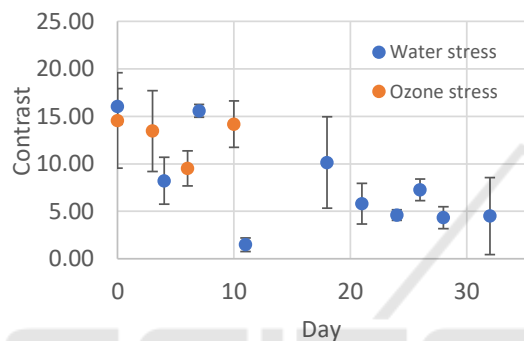

（a）Contrast

(b) Correlation

(c) Homogeneity

Figure 8: The result of GLCM.

Homogeneity increased during water stress(Fig.8(c)), while it showed little change under ozone stress. After watering was resumed, the value remained relatively constant. The Homogeneity value rises when adjacent pixels have similar intensity pairs. During water stress, the Homogeneity value changes due to similar reasons as those affecting Contrast.

The GLCM values exhibited different trends of change between the two types of stress, similar to the variations observed in the intensity and thickness of the palisade tissue; however, these changes were not as significant. Therefore, to enhance the visibility of changes in the texture analysis using GLCM related to the intensity and thickness change, it is necessary to apply specific image processing techniques such as preprocessing. Nevertheless, the results indicate that the internal changes in the leaves of *Trifolium repens* exposed to environmental stress can be categorized according to the type of stress experienced.

4 CONCLUSION

In this study, we apply OCT (Optical Coherence Tomography) measurement as a method for evaluating indicator plants to estimate the state of environmental pollution. To monitor the ozone pollution, which has been exacerbated by the development of automobile-based societies, we conducted OCT measurements on the leaves of *Trifolium repens* grown under different conditions. To quantify changes specific to ozone stress evaluated in OCT images, we also measured changes due to water stress for comparison. For quantitative analysis, we analyzed the interference light intensity, thickness, and texture (Contrast, Correlation, Homogeneity) in the palisade tissue.

Although differences between each type of stress were not clearly visible in the OCT images, changes in the intensity and thickness of the palisade tissue were estimated quantitatively. Changes were also observed in the texture analysis results (Contrast, Correlation, Homogeneity), but these changes were not as significant as those in intensity and thickness. It is possible that more distinct changes could be deduced by applying image processing techniques to make the intensity differences within the image clearer or by changing the direction in which the GLCM (Gray Level Co-occurrence Matrix) analysis is performed.

From these results, it can be concluded that different changes occur in the palisade tissue due to ozone stress and water stress, and that it is possible to classify these changes using OCT measurements. By

further advancing detailed research on the influence of different stresses on leaves, it will become possible to accurately identify the cause of stress using OCT. OCT can be taken to the on-site where plants are grown for measurements, allowing for quick, real-time, and in vivo estimation of the environmental conditions on the site. This study demonstrates the potential to estimate the environmental conditions to which plants are exposed, which could be beneficial in agricultural production environments.

ACKNOWLEDGMENTS

REFERENCES

Colston, B. W., Sathyam, U. S., DaSilva, L. B., Everett, M. J., Stroeve, P., & Otis, L. L. (1998). Dental OCT. Optics Express, 3(6), 230.

Fercher, A. F., Drexler, W., & Hitzenberger, C. K. (1996). OCT techniques (R. Birngruber, A. F. Fercher, & P. Sourdille, Eds.; pp. 164–174).

Goto, H., Lagrosas, N., Galvez, M. C., Vallar, E., & Shiina, T. (2024). Depth enlargement and homogenization from plant-OCT observations by using optical clearing. Optik, 316, 172065.

Goto, H., Lagrosas, N., & Shiina, T. (2024). OCT Image Analysis of Internal Changes in Leaves due to Ozone Stresses. Proceedings of the 12th International Conference on Photonics, Optics and Laser Technology, 65–71.

Goto, H., & Shiina, T. (2023). Environmental Pollution Assessment with Indicator Plant Under Ozone Gas Atmosphere by Using OCT. Proceedings of the 11th International Conference on Photonics, Optics and Laser Technology, 34–39.

Kitao, M., Löw, M., Heerdt, C., Grams, T. E. E., Häberle, K.-H., & Matyssek, R. (2009). Effects of chronic elevated ozone exposure on gas exchange responses of adult beech trees (Fagus sylvatica) as related to the within-canopy light gradient. Environmental Pollution, 157(2), 537–544.

Lee, J., Lee, S.-Y., Wijesinghe, R. E., Ravichandran, N. K., Han, S., Kim, P., Jeon, M., Jung, H.-Y., & Kim, J. (2019). On-Field In situ Inspection for Marssonina Coronaria Infected Apple Blotch Based on Non-Invasive Bio-Photonic Imaging Module. IEEE Access, 7, 148684–148691.

Li, M., Rivera, S., Franklin, D., Nowak, E., Hallett, I., Kolenderska, S., Urbańska, M., Vanholsbeeck, F., & East, A. (2021). Use of optical coherence tomography and light microscopy for characterisation of mechanical properties and cellular level responses of 'Centurion'

blueberries during weight loss. Journal of Food Engineering, 303, 110596.

Li, X., Yang, X., Li, X., Zhao, Z., Zhang, Z., Lin, H., Kang, D., & Shen, Y. (2022). Nondestructive in situ monitoring of pea seeds germination using optical coherence tomography. Plant Direct, 6(7).

Liu, Y., Zhu, D., Xu, J., Wang, Y., Feng, W., Chen, D., Li, Y., Liu, H., Guo, X., Qiu, H., & Gu, Y. (2020). Penetration-enhanced optical coherence tomography angiography with optical clearing agent for clinical evaluation of human skin. Photodiagnosis and Photodynamic Therapy, 30, 101734.

Oishi, Y. (2018). Comparison of moss and pine needles as bioindicators of transboundary polycyclic aromatic hydrocarbon pollution in central Japan. Environmental Pollution, 234, 330–338.

Osakabe, Y., Osakabe, K., Shinozaki, K., & Tran, L.-S. P. (2014). Response of plants to water stress. Frontiers in Plant Science, 5.

Pell, -Eva J., Schlagnhaufer, C. D., & Arteca, R. N. (1997). Ozone-induced oxidative stress: Mechanisms of action and reaction. Physiologia Plantarum, 100(2), 264–273.

Schneider, H., Park, K.-J., Häfer, M., Rüger, C., Schmalz, G., Krause, F., Schmidt, J., Ziebolz, D., & Haak, R. (2017). Dental Applications of Optical Coherence Tomography (OCT) in Cariology. Applied Sciences, 7(5), 472.

Sharifi, F., Naderi-Boldaji, M., Ghasemi-Varnamkhasti, M., Kheiralipour, K., Ghasemi, M., & Maleki, A. (2023). Feasibility study of detecting some milk adulterations using a LED-based Vis-SWNIR photoacoustic spectroscopy system. Food Chemistry, 424, 136411.

Srivastava, V., Dalal, D., Kumar, A., Prakash, S., & Dalal, K. (2018). In vivo automated quantification of quality of apples during storage using optical coherence tomography images. Laser Physics, 28(6), 066207.

Tewarie, P., Balk, L., Costello, F., Green, A., Martin, R., Schippling, S., & Petzold, A. (2012). The OSCAR-IB Consensus Criteria for Retinal OCT Quality Assessment. PLoS ONE, 7(4), e34823.